Analysis of Stress in PD Front End Solenoids

I. Terechkine

I. Introduction.

There are four different types of superconducting solenoids used for beam focusing in the Frond End of the Proton Driver. Table 1 gives an idea about requirements for certain parameters of the solenoids (some question marks in the table reflect lack of understanding of the situation with the available space at the moment).

Table 1

	DTL	MEBT	SSR	DSR
Parameter				
Bore diameter	25 mm	25 mm	30 mm	30 mm
Bore type	warm	warm	cold	cold
Field Integral FI = $\int B^2 dl$ ($T^2\cdot$cm)	218	264	313	478
Recommended Bm (T)	5	5.5	6	5.4
Leff (cm) @ Bm	9.78	9.78	9.78	17.66
Available insertion gap (cm)	25 (18 ?)	(18 ?)	39 (18 ?)	30 (32 ?)

The central magnetic field is in the range (5 – 6) T when longitudinal field profile is quasi-rectangular. In real situation, this is far from being true, and to reach required Field Integral (FI) within available space and with sufficient margin for stable work, magnetic field strength in the coil in some cases must be as high as ~8.5 T. With this field level, stress developed in the system leads to deformation that can result in coil boundary separation and subsequent coil quenching. Traditional method of solving this problem is applying to the problem some of known techniques of stress management. Methods of the stress management must be analyzed in conjunction with the solenoid assembly technique before prototypes of the devices are built. A convenient mean of stress analysis during this development stage would be very useful to accelerate the process of material and geometry choice. After this choice is made, traditional means of stress analysis, like using ANSIS code, can be used for verification of stress management solution and adjustment of design features.

Because of relatively simple geometry of the solenoids, which are axially symmetrical, it is possible to employ general methods of analysis based on direct solution of differential equations that describe mechanical behavior of the system. In spite of its axial symmetry, in the radial direction structure of the solenoids can be quite complex and usually includes beam pipe, bobbin, epoxy-impregnated coil (maybe several layers, separated by additional “protection” shells), a collar, and a steel yoke. Besides, during winding stage, inevitable wire tensioning provides additional pre-stress, that must be taken into the account. As a result, system of equations describing the system becomes quite large, and difficult for direct analysis. Nevertheless, with some simplifications, this system of equations can be solved using MathCad environment, visualized, and analyzed.

This note provides a description of the approach to the analysis of stress management solution for superconducting solenoids. Examples in this note do not reflect real design of any of mentioned solenoid; they rather help to illustrate certain aspects of the approach.

II. Basic Equations

Description of mechanical behavior of any solid media is based on equations of equilibrium and elasticity. Equilibrium condition in a cylindrical system with volume force of any nature can be written as:

$$\frac{d}{dr}(r\sigma_n) = \sigma_t - rF(r), \qquad /1/$$

where σ_n is normal stress, σ_t is tangential stress, and F(r) is an external force applied to a unit of volume (e.g. 1.0 m^3) of the material.

Elasticity equations describe deformation of material subject to normal and tangential stress:

$$\begin{aligned} \frac{u}{r} &= \frac{\sigma_t - \mu\sigma_n}{E}, \\ \frac{du}{dr} &= \frac{\sigma_n - \mu\sigma_t}{E} \end{aligned}, \qquad /2/$$

where μ is Poisson's ratio.

Combining /1/ and /2/, general equation of deformation can be obtained:

$$\frac{d^2u}{dr^2} + \frac{1}{r}\frac{du}{dr} - \frac{u}{r} = -\frac{1-\mu^2}{E}F(r) \qquad /3/$$

General solution of the homogeneous part of this differential equation (volumetric force is zero) is well known [1]:

$$u_h = C1 \cdot r + \frac{C2}{r}, \qquad /4/$$

where C1 and C2 are constants that can be found by analyzing boundary conditions.

To find a particular solution of the non-homogeneous equation /3/, we need to know what the volumetric force F(r) looks like. In the case of magnetic force,

$$\vec{F}(r) = \vec{j} \times \vec{B}(r) \qquad /5/$$

where $\boldsymbol{j}$ (A/m^2) is current density in the coil winding.

Radial profile of magnetic field inside the body of the coil in solenoids is close to linear, and in the median plane only z-component exists, so we will approximate it using the next form:

$$B(r) = B_i \cdot \frac{(1-\alpha\beta) - {}^{r}\!/_{R_o} \cdot (1-\beta)}{1-\alpha} \qquad /6/$$

where $\alpha = R_i/R_o$ is the ratio of inner and outer radii R_i and R_o, and $\beta = B_o/B_i$ is a ratio of magnetic field levels on the outside and inside border of a particular layer. As it is easy to check, $B(R_i) = B_i$, and $B(R_o) = \beta B_i$.

Value of B_i must be found for each layer by solving corresponding magnetostatic problem analytically (e.g. see [2]) or by using an appropriate solver. In our case, it is convenient to represent this value of magnetic field on the inside border of layer "*n*" by writing:

$$B_{i,n} = K_n \cdot I, \qquad /7/$$

where I is wire current. This current is usually kept constant even if wire diameter is different for different layers.

Introducing wire cross-section area S_w and coil compaction factor $k = S_w/S_c$, we can write down expression for the volumetric force (for each current-carrying layer):

$$F(r) = \frac{kK}{S_w} \cdot I^2 \cdot \left[\frac{1-\alpha\beta}{1-\alpha} - \frac{r}{R_o} \frac{1-\beta}{1-\alpha} \right] \qquad /8/$$

Then, now non-homogeneous equation /3/ looks like

$$\frac{d^2u}{dr^2} + \frac{1}{r}\frac{du}{dr} - \frac{u}{r^2} = -C0_1 + C0_2 \frac{r}{R_o} \qquad /9/$$

with $C0_1 = \frac{1-\mu^2}{E} \cdot \frac{kKI^2}{S_w} \cdot \frac{1-\alpha\beta}{1-\alpha}$, and $C0_2 = \frac{1-\mu^2}{E} \cdot \frac{kKI^2}{S_w} \cdot \frac{1-\beta}{1-\alpha}$.

Partial solution of equation /9/ can be found as:

$$u_p = -\frac{1}{3} C0_1 \cdot r^2 + \frac{1}{8R_o} C0_2 \cdot r^3 \qquad /10/$$

Then the general solution of this equation is:

$$u = C1 \cdot r + \frac{C2}{r} - \frac{1}{3} C0_1 \cdot r^2 + \frac{1}{8R_o} C0_2 \cdot r^3 \qquad /11/$$

So, for each layer of the solenoid (with or without current), equation /11/ gives an analytical solution for deformation. All the coefficients in equations /9/ ÷ /11/ are unique for each layer. $C0_1$ and $C0_2$ become known when coil dimensions are postulated; C1 and C2 must be found for each layer by applying corresponding boundary conditions, which usually means knowing stress or stress relationship on boundaries.

Knowing $\boldsymbol{u}$, normal and tangential (hoop) stress can be derived from /2/:

$$\sigma_n = \frac{E}{1-\mu^2} \left(\frac{du}{dr} + \mu \frac{u}{r} \right) \qquad /12/$$

and

$$\sigma_t = \frac{E}{1-\mu^2} \left(\frac{u}{r} + \mu \frac{du}{dr} \right) \qquad /13/$$

By combining /11/, /12/, and /13/, we get quite general analytical expressions for normal and tangential stress in any layer of the solenoid:

$$\sigma_n(r) = \frac{E}{1-\mu^2} \left[C1 \cdot (1+\mu) - \frac{C2}{r^2} \cdot (1-\mu) - \frac{C0_1}{3} \cdot r \cdot (2+\mu) + \frac{C0_2}{8R_o} \cdot r^2 \cdot (3+\mu) \right] \qquad /14/$$

$$\sigma_t(r) = \frac{E}{1-\mu^2} \left[C1 \cdot (1+\mu) + \frac{C2}{r^2} \cdot (1-\mu) - \frac{C0_1}{3} \cdot r \cdot (1+2\mu) + \frac{C0_2}{8R_o} \cdot r^2 \cdot (1+3\mu) \right] \qquad /15/$$

Now we can use /14 and /15/ to find unknown C1 and C2 for each layer "n" by solving a system of algebraic equations that define boundary conditions. This system is made by combining continuity equations for normal stress at the boundaries between layers "m" and "*m+1*":

$$\sigma_{m\_n} = \sigma_{m+1\_n} \qquad /16/$$

and interference equations at the same boundaries:

$$u_m - u_{m+1} = \delta \qquad /17/$$

Here $\boldsymbol{\delta}$ has sense of a gap between the two layers, so for overlapping layers it must be negative: $\delta < 0$. In other words, expression /17/ means that after assembly, the inner radius of the outer layer is equal to the outer radius of the inner layer:

$$R_{m+1} + u_{m+1} = R_m + u_m \text{ or } R_{m+1} = R_m + \delta. \qquad /18/$$

For any number of layers, we have sufficient amount of algebraic equations to find coefficients C1 and C2 for each layer.

One important practical aspect is that while assembling a multilayer solenoid, overlap can only be measured relatively to already assembled sub-structure. So, no readily available information exists about the "free state" overlap and means must be found to obtain this information. This evaluation will be a multi-step process repeated as many times as the number of layers is. Deformation $\boldsymbol{u}$ for any layer is defined relative to the "free" or undisturbed position if the layer, which often can not be measured directly.

An algorithm to find the "free state" overlap is described below.

Step 1: Adding layer #2 to the layer #1

R1o_0 is the outer radius of the layer #1 before adding the layer #2. For the layer #1 it is the same as the "free state" position. Initial inner radius of the layer #2

$$R2i\_0 = R1o\_0 + \delta 12. \qquad /19/$$

After the two layers are assembled, *R2i_1 = R1o_1.* At this step,

$$R2i\_1 = R2i\_0 + u2(R2i) = R1o\_0 + \delta 12 + u2(R2i) \qquad /20/$$

and

$$R1o\_1 = R1o\_0 + u1(R1o). \qquad /21/$$

Combining the last two equations, we come to what /17/ requires at the boundary between the two layers.

After solving the system of equations /14/ - /17/, we can find

$$R2o\_1 = R2o\_0 + u2(R2o). \qquad /22/$$

R2o_1 becomes a reference radius for determining the overlap between the layers #2 and #3. In the case of wound layers (see below), knowing *u2(R2o)* allows recalculation of a "free state" position of the layer's boundary.

Step 2: Adding layer #3 to the assembly (#1+#2)

Initial inner radius of the layer 3

$$R3i\_0 = R2o\_1 + \delta 23. \qquad /23/$$

Here overlap *δ23* is measured relatively to the position of the outer boundary of the layer #2 after it is added to #1. For stress evaluation, one need to know a "free state" overlap, that is the overlap between the undisturbed matching boundaries of the layers:

$$\delta 23\_free = R3i\_0 - R2o\_0 = \delta 23 + u2(R2o) \qquad /24/$$

Now we have three layers with two unknown coefficients defining deformation in each of them. So, we need six equations to find a solution. Four equations will be made by defining normal stress at the boundaries (equations /16/), and two equations /17/ will state that boundaries of the interfering layers are fused together:

$$R2i\_2 = R1o\_2 \text{ and } R3i\_2 = R2o\_2.$$

When the system of equations is solved we know deformations in each layers, including the last one. This allows to find a reference radius for determining the overlap between the layers #3 and #4:

$$R3o\_2 = R3o\_0 + u3(R3o) \qquad /25/$$

The procedure can be repeated as many times as the number of layers is.

Although mathematically we can find a solution, it can be too vague if we do not exactly know property of all materials we are using to build a solenoid. Some of them are composite materials with anisotropic properties depending on a technique used for solenoid assembly, so it is necessary be very careful in using available data. Here we'll try to make preliminary estimate of what these properties can look like, but only proper prototyping can give us correct numbers. This is also true for thermal contraction coefficients of all materials. This kind of data is scarce and often unreliable for composite materials, so our own judgment is needed. Once material properties are known, one can use the model developed above to make several iterations approaching a solution by changing materials and geometrical parameters of a solenoid.

III. Composite materials in solenoid

Some areas of the assembled solenoid have anisotropic properties that depend on fabrication technique. These areas are a coil, which is wound using NbTi wire with some tension and after winding is impregnated with epoxy, and a separation/protection layer that is wound using fiberglass tape above the coil and also impregnated with epoxy. In both cases, wound layers of the coil are under tension and cured epoxy is not stressed. During cooling down or when pre-stress is applied, both wound base and cured epoxy work simultaneously to form a unified composite object.

In this part, relevant properties of composite structure will be evaluated based on known properties of used materials.

How the coil is wound has a big impact of what properties to expect. We will start with a regular layered winding pattern shown in Figure 1 below.

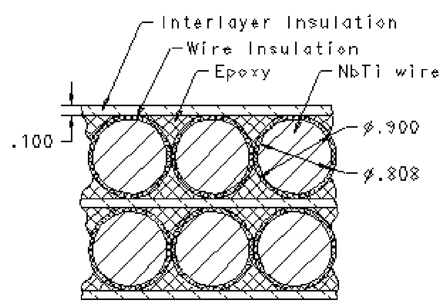

Figure 1: Structure of wound and impregnated coil. Pattern 1

Here, to create a base for winding each next layer, a relatively thick film must be used for layer separation. This structure suggests different mechanical properties along wire and across the layers of winding.

Along the length of wire (tangential direction) all parts of the coil cross section are acting in parallel, so effective elongation modulus of the structure in this direction is defined by relative area of NbTi wire and insulating material. If (for simplification) to accept that the three insulating materials used in the assembly have similar mechanical properties (that of cured epoxy), effective elongation modulus can be found as

$$E_t = \frac{E_w \cdot S_w + E_{ins} \cdot S_{ins}}{S_w + S_{ins}} \qquad /26/$$

Using E_w = 100 GPa, E_{ins} = 15 GPa, and taking wire and insulation dimensions from Figure 1, we get effective elongation modulus in GPa:

$$E_t = \frac{E_w \cdot \pi/4 \cdot D_{bare}^2 + E_{ins} \cdot \left[D_{ins} \cdot (D_{ins} + t) - \pi/4 \cdot D_{bare}^2\right]}{D_{ins} \cdot (D_{ins} + t)} = 63.4 \qquad /27/$$

Here D_{bare} and D_{ins} are diameters of bare and insulated strand. Compaction factor of this coil is **0.57**, so epoxy filling adds about 10% to what winding without filling would show when stretched. Presence of epoxy is crucially important when coil is under compression: epoxy filling and bonding insures that the structure behaves like a solid body.

Across the layers of winding (in normal direction) there is more complicated combination of interaction patterns. The ratio of the component cross-sections changes continuously in the normal direction (coordinate h). We will evaluate properties of this composite by analyzing serial connection of many thin layers with cross section shared by wire and insulation (see Figure 2). In each layer, effective elongation modulus, as before, is defined by relative area of the two components of the structure that act in parallel (simplification again), so this effective modulus varies in the normal direction.

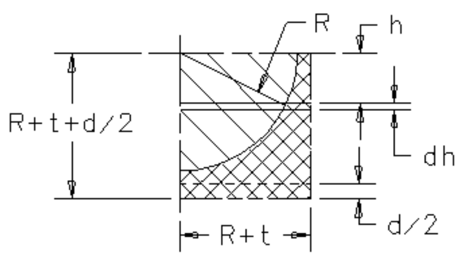

Figure 2: Illustration to evaluation of mechanical properties of coil structure in transverse direction

Taking into the account /26/, and all variable designations from Figure 2, we can write down:

$$E_{eff}(h) = \frac{E_w \cdot R \cdot \sqrt{1 - h^2/R^2} + E_{ins} \cdot \left[t + R \cdot (1 - \sqrt{1 - h^2/R^2})\right]}{R + t} \quad \text{if } h \le R \qquad /28\text{-a}/$$

and

$$E_{eff}(h) = E_{ins} \quad \text{if } h > R \qquad /28\text{-b}/$$

Global elasticity modulus can be found by taking integral:

$$\frac{1}{E_{e\Sigma}} = \frac{1}{R + t + d/2} \cdot \int_0^{R+t+d/2} \frac{dh}{E_{eff}(h)} \qquad /29/$$

Evaluation using known properties of wire and epoxy with t = 46 μm and d = 100 μm gives $E_{e\Sigma} \approx$ 39 GPa.

Another mode of coil winding is possible when thin and flexible insulation is used between the layers of winding that can not prevent wires from finding there position in notches between wires of the previously wound layer (see Figure 3). The only function of this insulation is to provide additional protection against shorts in the coil during cooling down:

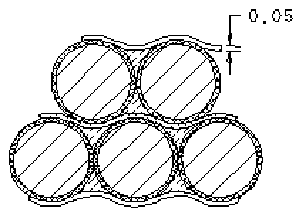

Figure 3: Structure of wound and impregnated coil. Pattern 2

This way higher density of winding can be obtained, that results in higher average elasticity modulus. This modulus can be evaluated as it was done for the pattern 1, but instead of using "*t+d/2*" in Figure 2 and integral expression, one must use "*d*" (see Fig. 4), that can be found geometrically and depends on the insulation thickness, which is shown as being 50 μm in Figure 3. With this insulation thickness, d = 14.3 μm if the rest of the parameters correspond to what was used for the previous case of "Pattern 1 winding".

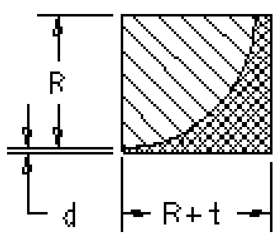

Figure 4: Pattern 2 cell used for average elasticity modulus evaluation.

Calculations using /28/ and /29/ give in this case elasticity modulus in transverse direction of ~58 GPa.

In the azimuthal direction, along wires, one must apply /26/ to find in GPa:

$$E_t = \frac{E_w \cdot \pi/4 \cdot R_{bare}^2 + E_{ins} \cdot \left\lfloor (R+t)\cdot(R+d) - \pi/4 \cdot R_{bare}^2 \right\rfloor}{(R+d)\cdot(R+t)} = 72.6 \qquad /30/$$

Compaction factor in this case is ~ 0.68.

Results of this analysis can be compared with test results in [3] on epoxy impregnated coils made of Nb_3Sn and NbTi using wire with rectangular cross-section. Elongation module was measured in the range 66 – 75 GPa. Other work of the same authors from NHMFL, [4], also provides some data related to mechanical behavior of wound coils. With packing factor of 0.8 (compare with 0.56 and 0.68 in our case), average modulus for coil stretching was ~ 95 GPa. For coil compression in radial direction, average modulus was only ~ 50 GPa.

Results of this simple analysis and existing data show that attention must be paid to how coil is fabricated.

Another note: If winding with glass tape and subsequent impregnation with epoxy is used above the coil, similar considerations can be used to find properties of the compound material. Reliable glass tape (strand) strength and density information is needed to make this work having sense. As a first approach, G-10 in the ward direction data can be used.

IV. Effects of cooling down

At room temperature, dimensions of all parts in the solenoid can be well controlled before they are added to the assembly. After several concentric parts are assembled together with some overlap, one does not have immediate control on the dimension of parts because of deformation (although dimensions still can be calculated).

We will assume that the outer surface of each part is machined after it is added to the assembly; so that the "as assembled" outer diameter is known every time. Then the required inner radius of the next part can be found using /18/ if the overlap $\boldsymbol{\delta}$ between the two layers is postulated.

The equations /16 and /17/, that model the assembly and are described above, are based on the differential equation for deformation /3/. As a result, there is no need to calculate exact values of radii; slight change of the radius of each boundary adds a correction to the result proportional to *u/R*. The value of overlap $\boldsymbol{\delta}$ is important though because it defines the initial deformation. So, the goal is to find new values of overlap for each couple of layer after cooling down.

One of ways of doing it is to use results of the stress analysis at room temperature that provides us with knowledge of the "free" dimensions of each layer after we find corresponding values of deformation. Knowing the "free" or undisturbed positions, we can apply to them the known thermal contraction properties to find undisturbed dimensions at 4 K. It is straightforward then to find overlap at each boundary and proceed to solving the system of equations /14/ - /17/ with (maybe) modified structural properties of used materials.

Another way is to reevaluate overlap information based on the "free" overlap data known from the room temperature case. For the interference between the layers *m* and *n*, one can write, similar to /17/:

$$\delta_{mn}^{(4K)} = R_{ni}^{(4K)} - R_{mo}^{(4K)} = R_{ni\_free}^{(300K)} \cdot (1-\chi_n) - R_{mo\_free}^{(300K)} \cdot (1-\chi_m)$$

or

$$\delta_{mn}^{(4K)} \approx \delta_{mn} - R_{mo}^{(300K)} \cdot (\chi_n - \chi_m) \qquad /31/$$

where χ_m and χ_n are integrated contraction coefficients of the layers in the temperature range from 300 K to 4 K, R_{mo} is the outer radius of the inner part, and indexes "*mo*" and "*ni*" refer to the matching outer and inner radii of the layers *m* and *n*.

So, again, the only thing that is needed here is data of "free" overlap at room temperature that can be found as was described above.

After we know overlap data, the system of equations /14/ - /17/ must be solved only once to give all the information we need.

V. Effect of wire tensioning during winding.

Wire tensioning is imminent during winding. Question arises on what impact this tensioning has on the solenoid mechanical behavior and whether this tensioning can be useful while solving the stress management problem.

Let's consider a layer of wire wound with tension force ***F*** above the bobbin or previously wound layer. We can treat this winding process as adding a solid cylindrical layer to the existing structure with the overlap ***δ*** at room temperature that corresponds to the tension force:

$$\delta = -r \cdot \frac{F}{E_w \cdot S_w}, \qquad /32/$$

Where E_w is Young's modulus and S_w is cross-section area of the strand (**w**ire).

Each next layer will have different interference because of different radius *R* and (maybe) tension force *F*. For each wound layer, the same basic equation /3/ will work with similar set of boundary conditions. Material properties must be used carefully while solving these equations. At this stage, liquid epoxy or no epoxy is used, so only wire and interlayer insulation must be taken into the account while evaluating structural properties of wound layers. After epoxy is cured, new values of material properties and modified thermal contraction coefficient (see below) must be used to analyze stress after cooling down. The approach to stress calculation at room temperature developed in the previous chapters is fully applicable because at each winding step we know the outer radius of the last wound layer and the inner radius of the next layer.

During cooling down, because thermal properties of the layers of winding are identical, overlap will change only because of deformation change due to stress redistribution, so again the same algorithm can be used.

VI. Mechanical behavior of wound and epoxy impregnated coil

Thermal contraction of coil structure is the issue to pay attention to. If coil's wire is wound with tension and then impregnated with epoxy and cured, at room temperature cured epoxy is unstressed while the coil wire is stretched. So, new "equilibrium" inner radius at room temperature must be found that corresponds to the case when this layer of coil assembly is removed from a bobbin (or previous layer) it was assemble on. Knowing this radius allows one to find interference needed to calculate displacements and stress.

Average properties of the material can be found in a way similar to what was used in the chapter 3 above, so for each material we will use averaged value of elasticity modulus.

After winding a layer of wire with tension F, increase of radius is defined by /32/:

$$\frac{\Delta r_F}{r} = \frac{F}{E_W \cdot S_W}$$

When wound and cured layer is removed from the bobbin, it contracts releasing the tension until force equilibrium is reached between compressed epoxy filling and stretched wire. New equilibrium position can be found from equation:

$$\frac{\Delta r_{eq}}{r} \cdot E_W S_W = \frac{\Delta r_F - \Delta r_{eq}}{r} \cdot E_{ins} S_{ins} \qquad /33/$$

Here Δr_{eq} shows increase of inner radius of the wound coil with cured epoxy after it is removed from the bobbin it was wound on relative to that without epoxy; S_{ins} is insulation cross-section per one turn f the winding. From /33/:

$$\frac{\Delta r_{eq}}{r} = \frac{F}{E_W S_W (1 + \dfrac{E_W S_W}{E_{ins} S_{ins}})} \qquad /34/$$

At this position, remaining inner stretching force per wire is

$$F_r = \frac{F}{1 + \dfrac{E_W S_W}{E_{ins} S_{ins}}} \qquad /35/$$

and adjusted overlap

$$\delta = \Delta r_{eq} - \Delta r_F = \frac{-rF}{E_W S_W + E_{ins} S_{ins}} \qquad /36/$$

Mechanical behavior of the composite structure, namely displacement relative the new equilibrium position, can be derived based on the known properties of the components making the structure and the new equilibrium position. If displacement relative to this position is x, corresponding force can be calculated as:

$$\frac{x}{r} S_\Sigma E_{eff} = \frac{x + \Delta r_{eq}}{r} E_W S_W - \frac{\Delta r_F - (x + \Delta r_{eq})}{r} E_{ins} S_{ins} \qquad /37/$$

Using /31/, we can simplify this expression to write:

$$S_\Sigma E_{eff} = E_W S_W + E_{ins} S_{ins} \qquad /38/$$

that one could expect just looking at /36/.

VII. Thermal contraction of epoxy impregnated structures

For superconducting solenoids, it is also important to know thermal contraction properties of composite materials to calculate overlap at 4K. We can make an estimate using the approach similar to what was used above.

During cooling down, due to different coefficients of contraction of coil wire and epoxy, one can expect redistribution of internal stress and change of the equilibrium position of inner and outer radii.

At room temperature, inner radius of the coil in "free" condition is defined by the radius of the bobbin r_b, overlap δ, which is a function of wire tension ($r_w = r_b + \delta$), and the stretching force of compressed filling material (epoxy) with the inner radius of r_b (which is the outer radius of the bobbin).

After cooling down, "free state" dimensions of the winding and of the epoxy filling change:

$$r_w^{4K} = r_w(1 - \chi_w) = (r_b + \delta)(1 - \chi_w) \qquad /39/$$

and

$$r_{epo}^{4K} = r_b(1 - \chi_{epo}), \qquad /40/$$

New equilibrium position of the inner radius is common both for winding and for epoxy filling. Also internal force must be compensated, so

$$\frac{r_{eq}^{(4K)} - r_w^{(4K)}}{r_w^{(4K)}} = \frac{N_{\text{int}}}{S_W E_W}$$
$$\frac{r_{ep}^{(4K)} - r_{eq}^{(4K)}}{r_{ep}^{(4K)}} = \frac{N_{\text{int}}}{S_{ins} E_{ins}} \qquad /41/$$

where N is the internal force of interaction between wire and epoxy filling.

Using /39/, /40/, and /41/, and taking into the account /32/, we get the next expression for the new equilibrium radius at 4 K:

$$r_{eq}^{(4K)} \approx r_b \left[1 - \frac{S_W E_W \chi_w + S_{ins} E_{ins} \chi_{ins} + F}{S_W E_W + S_{ins} E_{ins}} \right] \qquad /42/$$

The second term in the parentheses above is the effective integrated thermal contraction coefficient of a composite material. As before, S_{ins} includes not only epoxy, but also interlayer insulation. Young's modulus E_W of the strand must be taken for the longitudinal direction because we deal here with layer elongation that translates into corresponding radius change.

Using typical data one can get:

$S_w E_w \approx 50 \cdot 10^3$ N, $\chi_w = 1.9 * 10^{-3}$

$S_{ins} E_{ins} \approx 6 \cdot 10^3$ N, $\chi_{ins} = 4.3 * 10^{-3}$

$S_w E_w \chi_w + S_{ins} E_{ins} \chi_{ins} \approx 120$ N,

which is comparable with the tension force usually used during winding. So, wire tension can modify material shrinkage in the case when epoxy is used as a filler material.

For sure, coil winding pattern (compaction factor) will modify numbers shown above. Taking into the account compaction factor, expression for the effective shrinkage coefficient can be written in the form:

$$\chi_{eff} = \frac{\chi_w + \frac{1-k}{k} \cdot \chi_{ins} \cdot \frac{E_{ins}}{E_w} + \frac{F}{E_w \cdot S_w}}{1 + \frac{1-k}{k} \cdot \frac{E_{ins}}{E_w}} \qquad /43/$$

For k = 0.63, with F ≈ 50 N, effective shrinkage $\chi_{eff} \approx 3.5 \cdot 10^{-3}$. With F ≈ 0, effective shrinkage $\chi_{eff} \approx 2.6 \cdot 10^{-3}$

If the coil spool is made of stainless steel ($\chi \approx 3 \cdot 10^{-3}$), it would be a good idea to apply some tension to wire not to lose stress during cooling down.

VIII. Conclusion

This note forms a base for stress analysis of superconducting solenoids:

1. Basic equations were derived to analyze stress and deformations;
2. Expressions were found to estimate mechanical properties of composite materials like wound and epoxy impregnated Nb-Ti coil;
3. Algorithm of stress analysis at LHe temperature was suggested;
4. Method of stress analysis when wire tension is used during winding was suggested
5. Thermal shrinkage of epoxy impregnated coil was analyzed to show that it depends on coils winding patterns.

This set of algorithms will be applied and derived expressions will be used to make a choice of materials and assembly techniques of superconducting focusing coils in the PD front end.

IX. References

[1] J.P. Den Hartog, Strength of materials, Dover Publications, Inc, N-Y,
[2] D. Bruce Montgomery, Solenoid magnet design. The magnetic and mechanical aspects of resistive and superconducting systems. Wiley-Interscience, NY, 1969.
[3] I. Dixon, et al. Axial Mechanical Properties of Epoxy Impregnated Superconducting Solenoids at 4.2 K, IEEE Trans. on Applied Superconductivity, v. 10, No. 1, March 2000
[4] I. Dixon, et al, Mechanical Properties of Epoxy Impregnated Superconducting Solenoids, IEEE Trans. on Magnetics, v. 32, No. 4, July 1996